Electronic Supplementary Material (ESI) for Physical Chemistry Chemical Physics.
This journal is © the Owner Societies 2016

Supplementary Information

Spectral Mapping of 3D Multi-cellular Tumor Spheroid: Time-resolved Confocal Microscopy

Saswat Mohapatra,†[a,b] Somen Nandi,†[c] Rajdeep Chowdhury,†[c] Gaurav Das, [a] Surajit Ghosh*[a,b] and Kankan Bhattacharyya*[c]

[a]Organic and Medicinal Chemistry Division, CSIR-Indian Institute of Chemical Biology, 4, Raja S. C. Mullick Road, Jadavpur, Kolkata-700032, West Bengal, India

[b]Academy of Scientific and Innovative Research (AcSIR), CSIR-Indian Institute of Chemical Biology Campus, 4 Raja S. C. Mullick Road, Kolkata 700 032, India

[c]Department of Physical Chemistry, Indian Association for the Cultivation of Science, Jadavpur, Kolkata 700032, India

AUTHOR INFORMATION

†Equal Contribution

Corresponding Author

*pckb@iacs.res.in, *sghosh@iicb.res.in

A. Confocal Images of 2D and 3D Spheroid Stained by CPM: HeLa and A549 Cell

In order to avoid the photo-damage of live cell by high power of laser (405 nm), we have recorded the confocal images at very low laser power ~ 100 nW. Confocal images of 2D cell and different layers of 3D spheroid (stained by CPM) are given below. Corresponding bright field images are also shown.

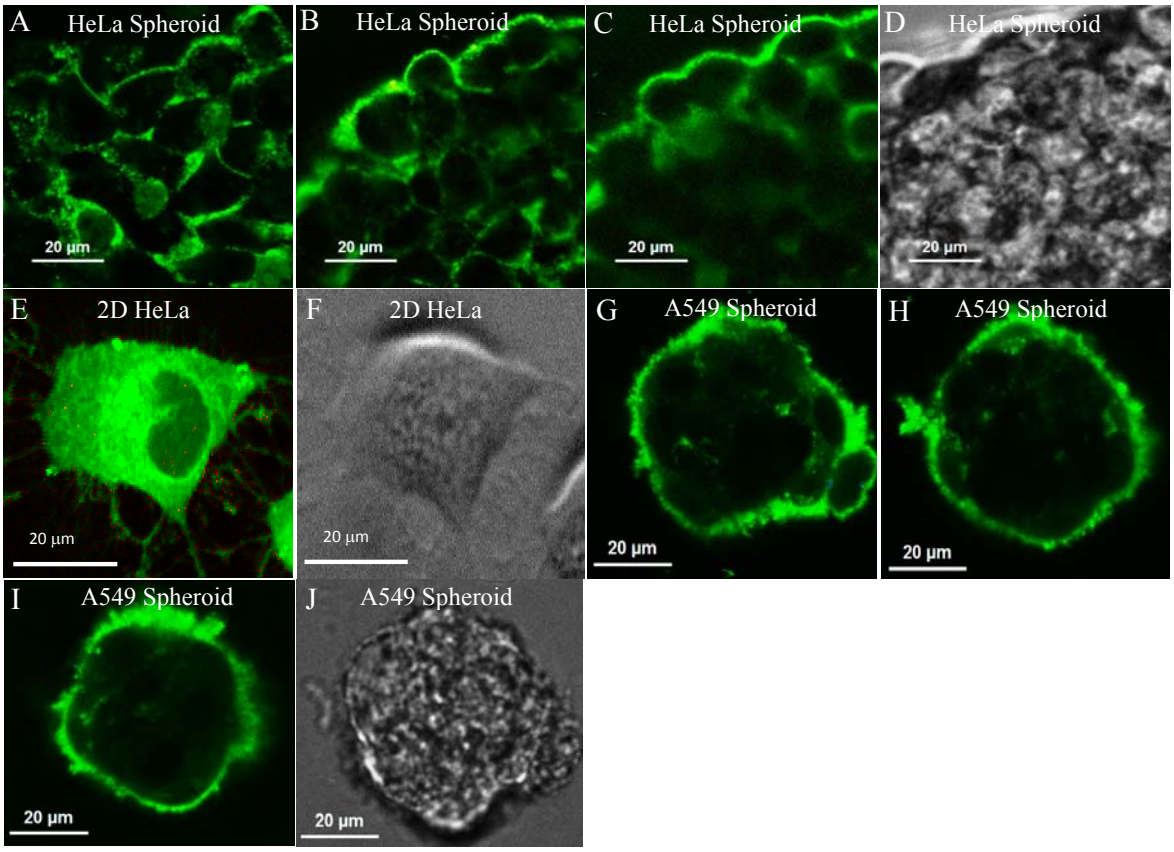

Figure S1. Confocal images- stained by CPM: Tumor spheroid of HeLa cell at (A) 0 µm, (B) 30 µm, (C) 60 µm, along *z*-axis and (D) bright field image; (E) 2D HeLa cell, (F) Corresponding bright field image of 2D HeLa cell. Tumor spheroid of A549 cell at (G) 10 µm, (H) 20 µm, (I) 30 µm, along *z*-axis and (J) bright field image;

B. Peri-nuclear Region of 2D HeLa: Co-localization with ER Tracker

Figure S2A-B show confocal images of HeLa cells stained with CPM and ER tracker, respectively. We have also recorded confocal image of HeLa cell stained by both CPM and ER tracker dyes and represented in Figure S2C. Figure S2B clearly shows that ER is clustered in the peri-nuclear region.[1-2] In the ER region, ER tracker displays an emission maximum at ~502 nm (Figure S2D). CPM is also found to reside in the peri-nuclear region of HeLa cell (Figure S2A) and exhibits an emission maximum at ~473 nm. Since the emission maxima of CPM and ER tracker are very close, it is impossible to separate the emissions from CPM and ER tracker residing in the peri-nuclear region of same HeLa cell (Figure

S2C). However comparing the three confocal images, one may assume that the peri-nuclear region stained by CPM is ER. In order to prove this conclusively, we have recorded the emission spectra from the peri-clear region of a HeLa cell stained by both CPM and ER tracker (Figure S2C) and found an emission maximum ~ 485 nm which is in between that of CPM and ER tracker. Thus, we have concluded that the CPM is residing in the ER region clustered around the nucleus.

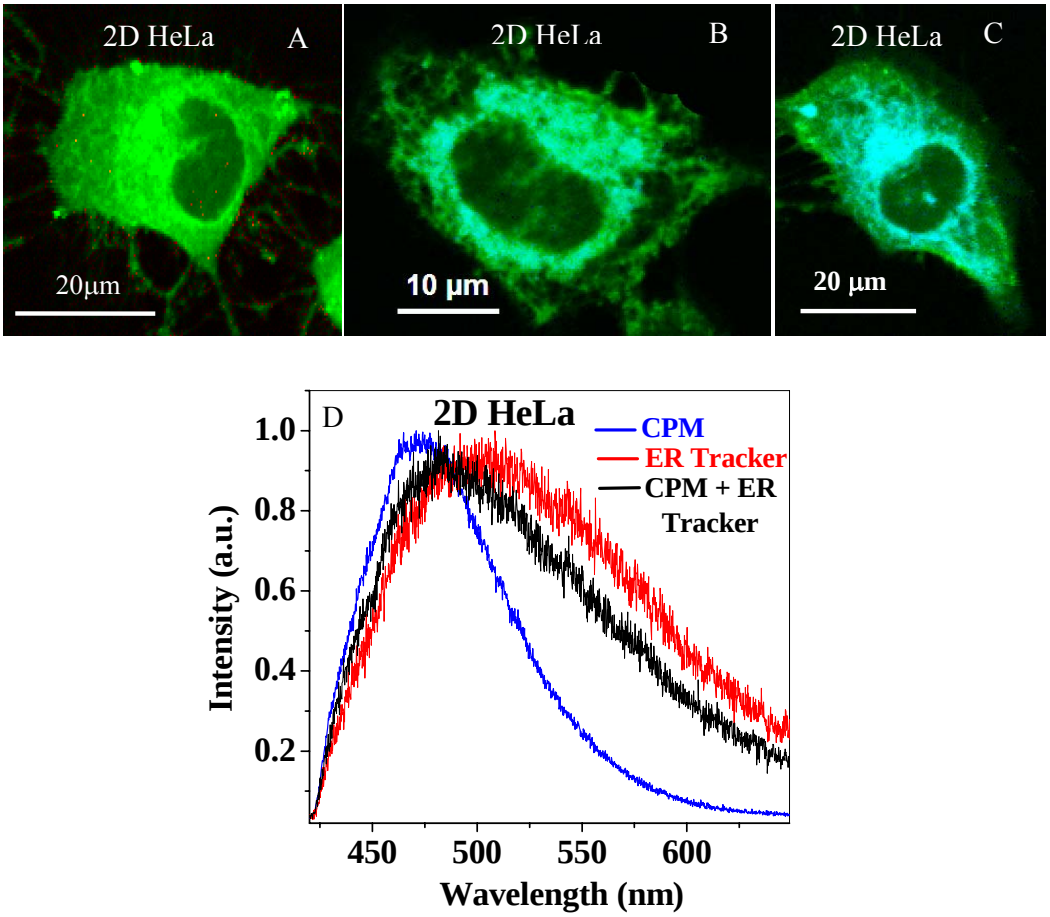

Figure S2. Confocal images of 2D HeLa cell stained by (A) CPM, (B) ER tracker and (C) both (CPM+ER tracker dye). (D) Emission spectra from the peri-nuclear region stained by CPM, ER tracker and both (CPM+ER tracker dye).

C. Confocal Images of 2D and 3D Spheroid Stained by C153: HeLa and A549 Cell

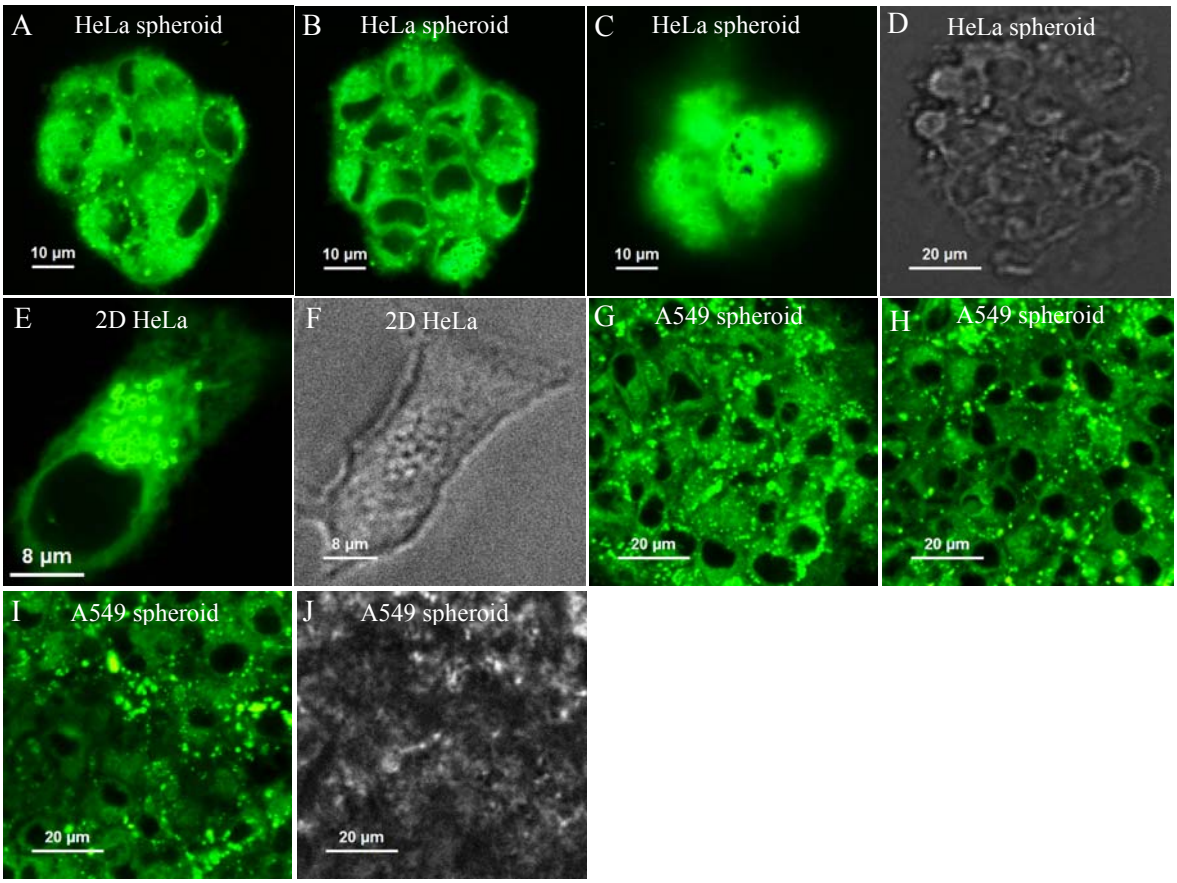

Figure S3. Confocal images- stained by C153: Tumor spheroid of HeLa cell at (A) 0 µm, (B) 20 µm, (C) 40 µm, along *z*-axis and (D) bright field image; (E) HeLa cell in 2D, (F) corresponding bright field image. Tumor spheroid of A549 cell at (G) 20 µm, (H) 30 µm, (I) 40 µm, along *z*-axis and (J) bright field image;

D. Confocal Images of 2D and 3D Spheroid stained by Dox: HeLa and A549 Cell

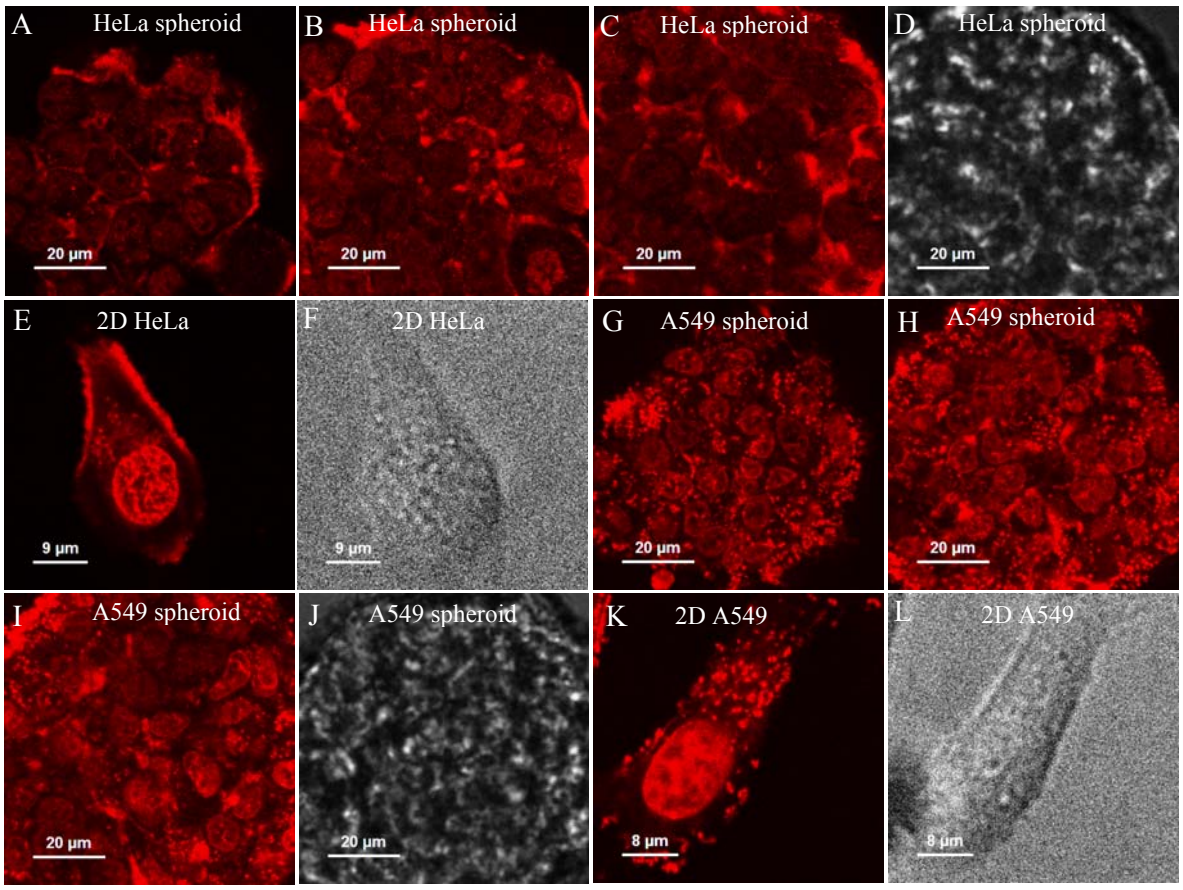

Figure S4. Confocal images- stained by Dox: Tumor spheroid of HeLa cell at (A) 10 µm, (B) 20 µm, (C) 30 µm, along *z*-axis and (D) bright field image; (E) 2D HeLa cell, (F) corresponding bright field image. Tumor spheroid of A549 cell at (G) 30 µm, (H) 40 µm, (I) 50 µm, along *z*-axis and (J) bright field image; (K) 2D A549 cell, (L) corresponding bright field image;

E. Confocal Images of 2D and 3D A549 Cells Stained by 1 μM Dox

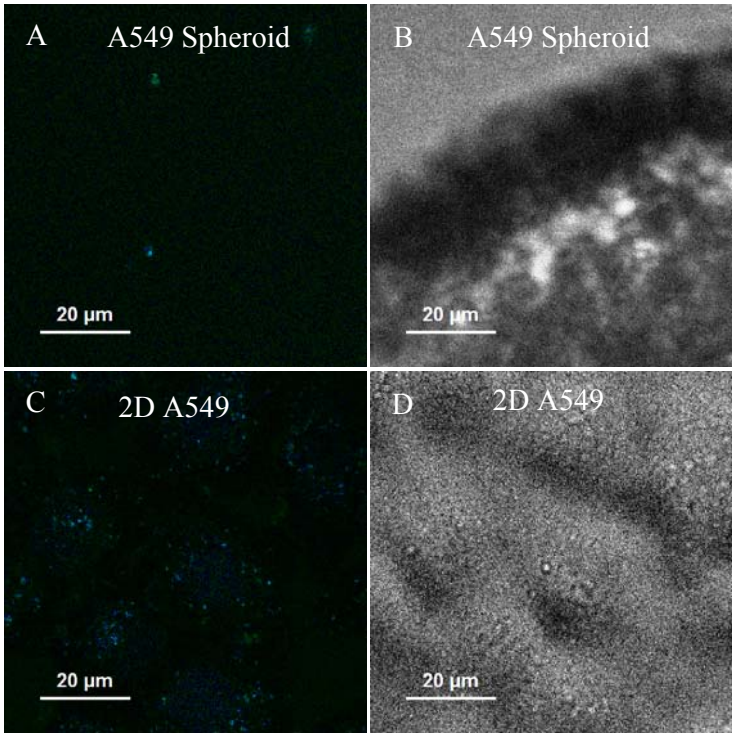

Figure S5. Confocal images- stained by 1 μM Dox: (A) A549 spheroid, (B) corresponding bright field image, (C) 2D A549 cell, (D) corresponding bright field image.

F. Distribution of Dox in both 2D and 3D Tumor of A549 Cells

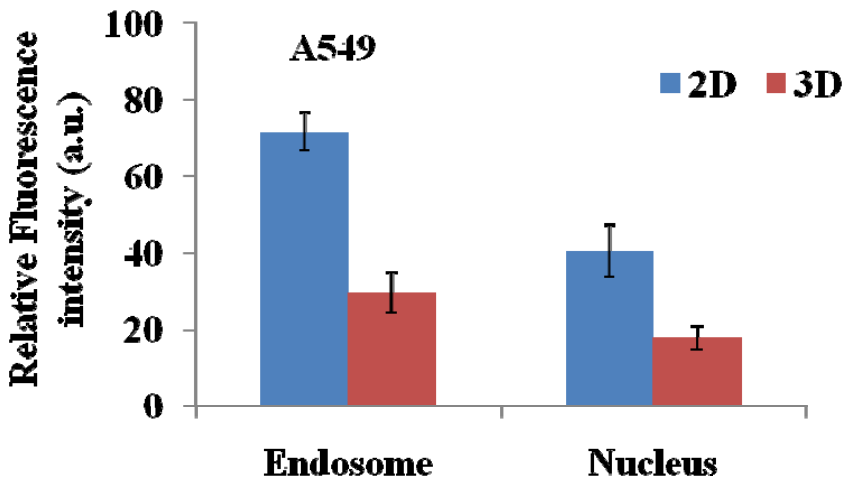

Figure S6. Distribution of Dox in A549 cells both in 2D and 3D cell culture system after treatment with 5 μM of Dox for 1 h.

G. Solvation Dynamics

Solvent correlation function (C(t)) may be defined as-

$$C(t) = \frac{\nu(t) - \nu(\infty)}{\nu(0) - \nu(\infty)} \qquad \text{(S1)}$$

where, ν(0), ν(t) and ν(∞) are the emission maxima (frequencies) at time 0, t and ∞, respectively. The denominator in the right hand side of equation S1 indicates total dynamic Stokes shift (Δν).

It may be noted here that the temporal resolution (IRF) of our picosecond set up is ~ 100 ps. Thus some amount of solvation dynamics occurring in <100 ps are missed. In order to detect the percentage of solvation missed, we have used Fee-Maroncelli equation[3] which may be given as-

$$\nu^{\mathbf{theo}}(\mathbf{0}) = \nu_{\mathbf{abs}}^{\mathbf{system}} - \left(\nu_{\mathbf{abs}}^{\mathbf{np}} - \nu_{\mathbf{em}}^{\mathbf{np}}\right) \qquad \text{(S2)}$$

$\nu^{theo}(0)$ in the above equation, denotes theoretical emission maximum at zero time. ν_{abs}^{np} and ν_{em}^{np} represents absorption and emission maxima, respectively of C153 in a non-polar solvent (cyclohexane). ν_{abs}^{system} indicates the absorption maximum of the system and could not be

obtained under the confocal microscope. ν_{abs}^{system} is assumed to be equal to the absorption maximum of C153 in a solvent where C153 display similar emission maximum as that in the live cell. Using this approximation, percentage missed is calculated using equation S2 and given in Table S1 and S2.

1. Non-covalent Probe (C153) in 2Dand 3D Cells: HeLa and A549

Figure S7 shows fluorescence transients of C153 in different regions of 2D HeLa and different layers of spheroid. Fluorescent transients display decays at short emission wavelength (at blue end) and rise preceding the decay at long emission wavelength (at red end). This clearly indicates that solvation dynamics is taking place.

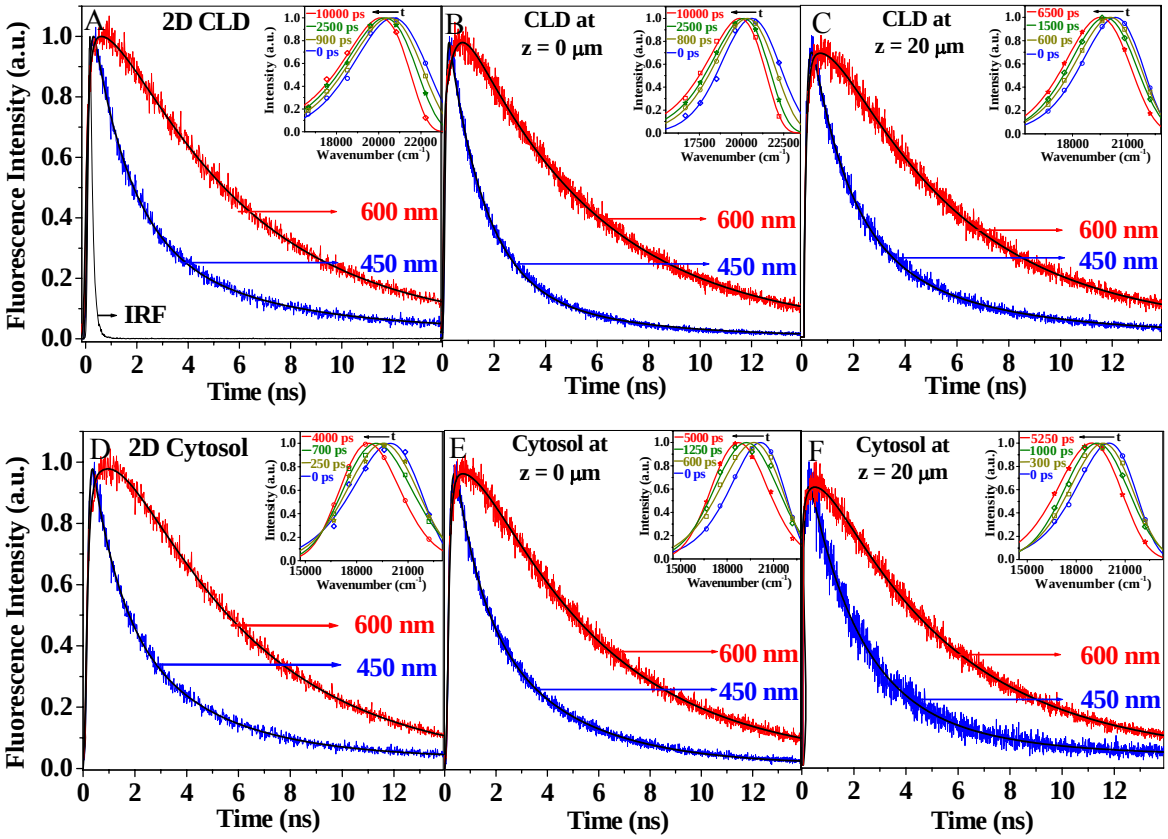

Figure S7. Fluorescence decays of C153. Inside the Lipid droplets: (A) 2D HeLa cell, (B) z=0 μm (bottom layer) of the tumor spheroid and (C) z=20 μm (upper layer) of the tumor spheroid. Inside the cytosol: (D) 2D HeLa cell, (E) z=0 μm (bottom layer) of the tumor spheroid and (F) z=20 μm (upper layer) of the tumor spheroid. Corresponding TRES are shown in insets.

Table S1. Decay parameter of solvent correlation function (C(t))

System (HeLa Cell)				$\Delta\nu$ [$\nu(0)$][a] cm^{-1}	$\nu(0)^{Theo}$ cm^{-1} (% missed)	τ_1 (a_1) ps	τ_2 (a_2) ps
Dye	Region		Height (z) μm				
C153	cytosol	2D	-	1273 [19958]	20285 (20)	500 (0.56)	1700 (0.24)
		Tumor spheroid	0	1408 [20150]	20285 (9)	1000 (0.91)	-
			20	1061 [20012]	20285 (20)	400 (0.48)	2300 (0.32)
	Lipid droplet	2D	-	582 [20682]	20982 (34)	1500 (0.26)	4000 (0.40)
		Tumor spheroid	0	709 [20602]	20982 (35)	800 (0.30)	5000 (0.35)
			20	824 [20329]	20718 (32)	1450 (0.68)	-
CPM	Perinuclear region	2D	-	259[b] [21433]	21555 (30)	800 (0.70)	-
	Membrane	Tumor spheroid	30	118[b] [21533]	21555 (15)	450 (0.50)	2000 (0.35)

[a] ± 100 cm^{-1}; [b] ± 20 cm^{-1}

Inside the cytoplasmic lipid droplets (CLDs) of 2D HeLa cell and bottom layer (z=0 μm) of spheroid, C153 exhibits a rise time of ~ 800 ps at the red end of the emission spectra (Figure S7A-B). On the other hand, the observed rise time is ~ 500 ps inside the CLDs of upper layer (z=20 μm).

The time resolved emission spectra (TRES) are constructed following the works of Maroncelli and Fleming[4-5] and presented in the inset of Figure S7. Total dynamic Stokes shift (DSS) calculated from the TRES and summarized in Table S1. In the CLDs of 2D HeLa cell, C(t) of C153 exhibits two components of solvation dynamics- 1500 ps (26%) and 4000 ps (40%). CLDs in bottom layer (z=0 μm) of spheroid display two components of solvation dynamics- 800 ps (30%) and 5000 ps (35%).

In contrast to the bottom layer (z=0 μm) of the spheroid, lipid droplets in the upper layer (z=20 μm) shows only one component of ~ 1450 ps (68%).

Wavelength dependent fluorescence decays of C153 in cytosol region are given in Figure S7D-F. At the red end of emission spectra, distinct rise (~350 ps) component is

detected in the cytosol of 2D HeLa and different layers of spheroid. TRES of C153 in the cytosol of 2D HeLa cell and spheroid are given in the inset of Figure S7D-F.

Fluorescence transients of C153 in different layers of A549 spheroid are shown in Figure S8. In contrast to the HeLa spheroid, inside the cytoplasmic lipid droplets (CLDs) of bottom layer (z=0 μm) of A549 spheroid, C153 exhibits a rise time of ~ 500 ps at the red end of the emission spectra (Figure S8A). On the other hand, inside the CLDs of upper layer (z=20 μm) of the spheroid, ~ 800 ps rise time is observed (Figure S8B).

Rise time of C153 in the cytosol of A549 spheroid is ~ 400 ps in all layers.

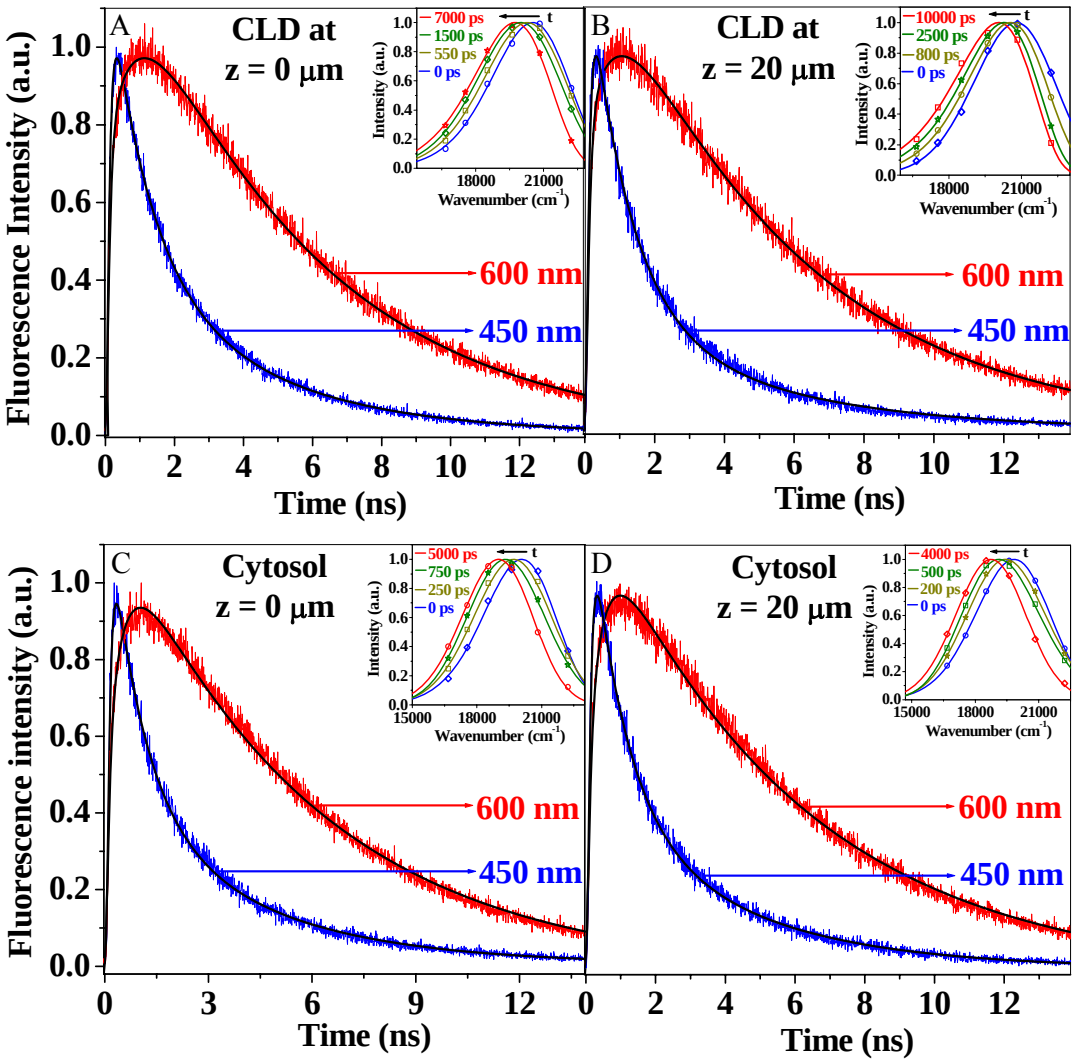

Figure S8. Fluorescence decays of C153 inside the A549 spheroid. Lipid droplets: (A) at z=0 μm (bottom layer) and (B) at z=20 μm (upper layer). Inside the cytosol: (C) at z=0 μm (bottom layer) and (D) at z=20 μm (upper layer). Corresponding TRES are shown in insets.

Table S2. Decay parameter of solvent correlation function (C(t))

System (A549 Cell)				$\Delta\nu$ [$\nu(0)$][a] cm^{-1}	$\nu(0)^{Theo}$ cm^{-1} (% missed)	τ_1 (a_1) ps	τ_2 (a_2) ps
Dye	Region		Height (z) μm				
C153	Cytosol	Tumor spheroid	0	1076 [20082]	20415 (24)	500 (0.58)	5000 (0.18)
			20	1079 [19834]	20285 (30)	360 (0.52)	5000 (0.18)
	Lipid droplet	Tumor spheroid	0	773 [20516]	20845 (30)	1350 (0.70)	-
			20	715 [20777]	20982 (22)	4000 (0.37)	1400 (0.41)
CPM	Membrane	Tumor spheroid	20	166[b] [21550]	21555 (3)	450 (0.58)	1600 (0.39)

[a] ± 100 cm^{-1}; [b] ± 20 cm^{-1}

The insets of Figure S8 represent the time resolved emission spectra (TRES). From the TRES, total dynamic Stokes shift (DSS) are calculated and summarized in Table S2. In the CLDs of A549 spheroid cell, C(t) of C153 exhibits single components of solvation dynamics- 1350 ps (70%) at bottom layer (z=0 μm). CLDs in upper layer (z=20 μm) of spheroid display two components of solvation dynamics- 1400 ps (41%) and 4000 ps (37%).

In the cytosol of A549 spheroid, C(t) exhibits two time components- 430±70 ps and 5000 ps.

2. Covalent probe (CPM) in 2D and 3D cells: HeLa and A549

Fluorescence transients of CPM are shown in Figure S9 and the inset shows corresponding TRES. Solvation dynamics is observed not to vary in different layers of the spheroid. Hence, we report the solvation dynamics data in only one layer (z=30 μm) of the tumor. It has already been mentioned that emission maxima of CPM in 2D cell and various layers of the spheroids are pretty close to that of CPM-labeled human serum albumin (HSA) in GdnHCl. Thus, it have been assumed that the $\nu^{theo}(0)$ of CPM in both of the cases (2D cell and 3D tumor) to be same as that for of CPM labeled HSA in 6 M guanidium hydrochloride (21 555 cm^{-1})[6]. Using this assumption, percentage of solvent missed are calculated. ~30% of

solvation dynamics is missed in case of 2D HeLa cell, whereas ~15% is missed in case of tumor spheroid, as shown in Table S1 and S2.

Total dynamic Stokes shift (DSS) are calculated from the TRES and summarized in Table S1 and S2. In the peri-nuclear region of 2D HeLa cell, C(t) of CPM displays a single component of solvation dynamics- 800 ps (70%) with an average solvation time (<τ_s>) of ~600 ps. On the other hand, C(t) of CPM in the membrane region of the HeLa spheroid (at z=30 μm) shows two time constants- 450 ps (50 %) and 2000 ps (35 %).

In the membrane region of A549 spheroid, decay of C(t) of CPM exhibits two time constants- 450 ps (58 %) and 1600 ps (39 %).

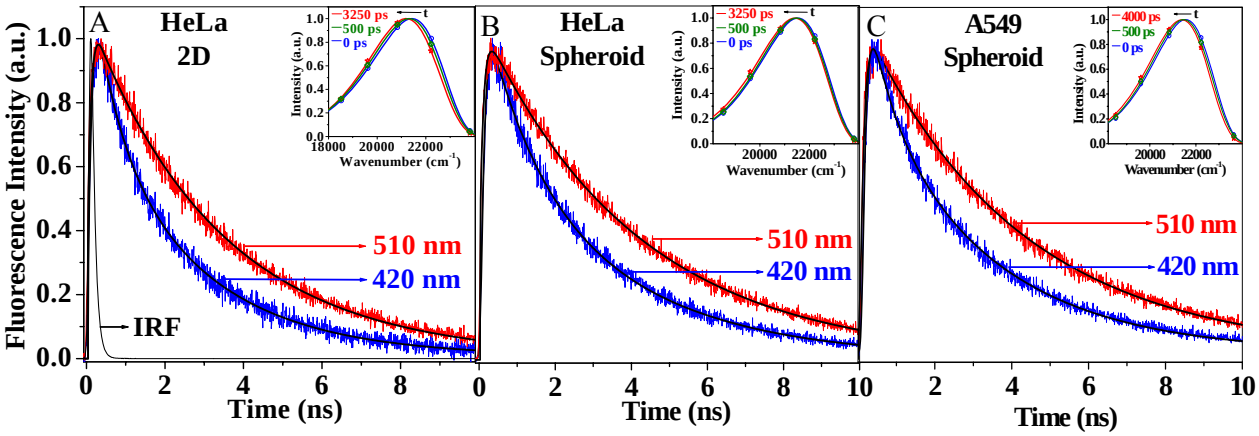

Figure S9. Fluorescence decays of CPM inside (A) the 2D HeLa cell, (B) HeLa spheroid (at z=30 μm) and (C) A549 spheroid (at z=20 μm) Corresponding TRES are shown in the insets.

H. Emission Spectra of C153 inside 2D and 3D (Spheroid) Cells: HeLa and A549

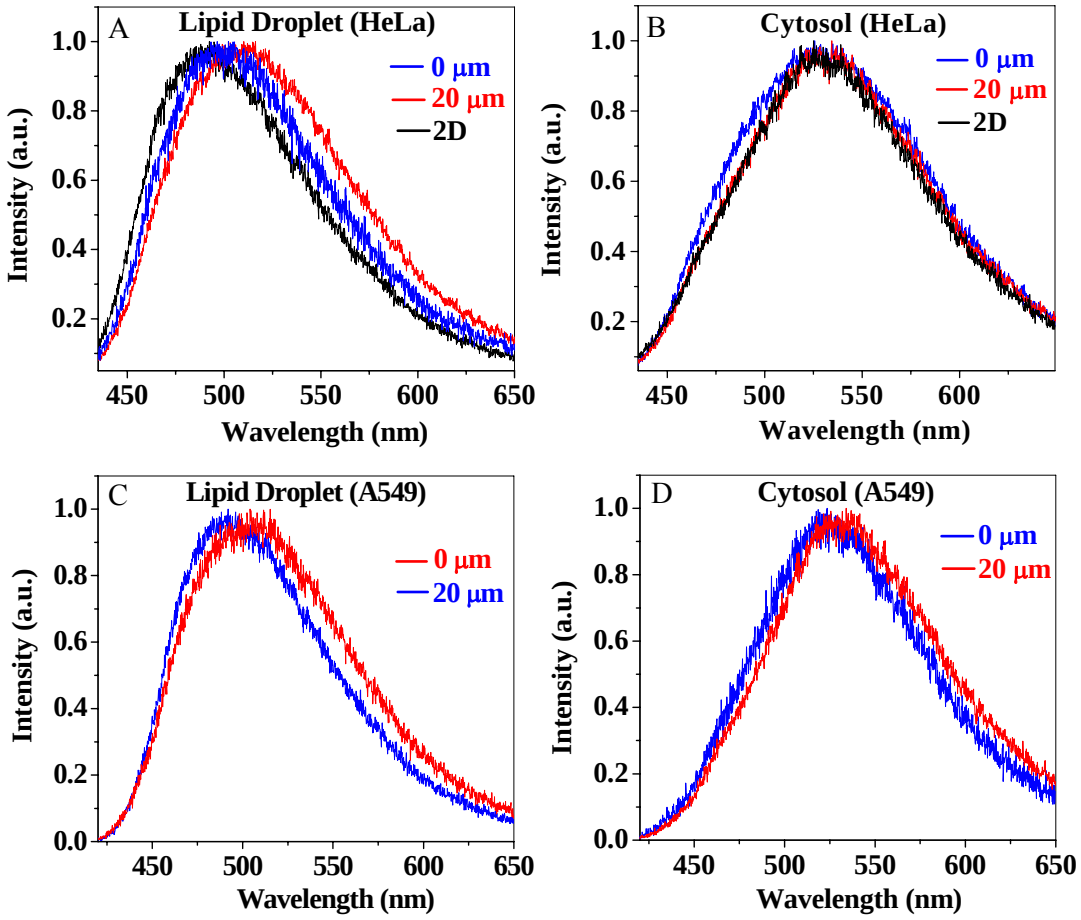

Figure S10. Emission spectra: HeLa cell - (A) inside the lipid droplet, (B) in the cytosol; A549 spheroid - (C) inside the lipid droplet, (D) in the cytosol, stained by C153.

I. Solvation Dynamics of C153 inside 2D and 3D (Spheroid) Cells: HeLa and A549

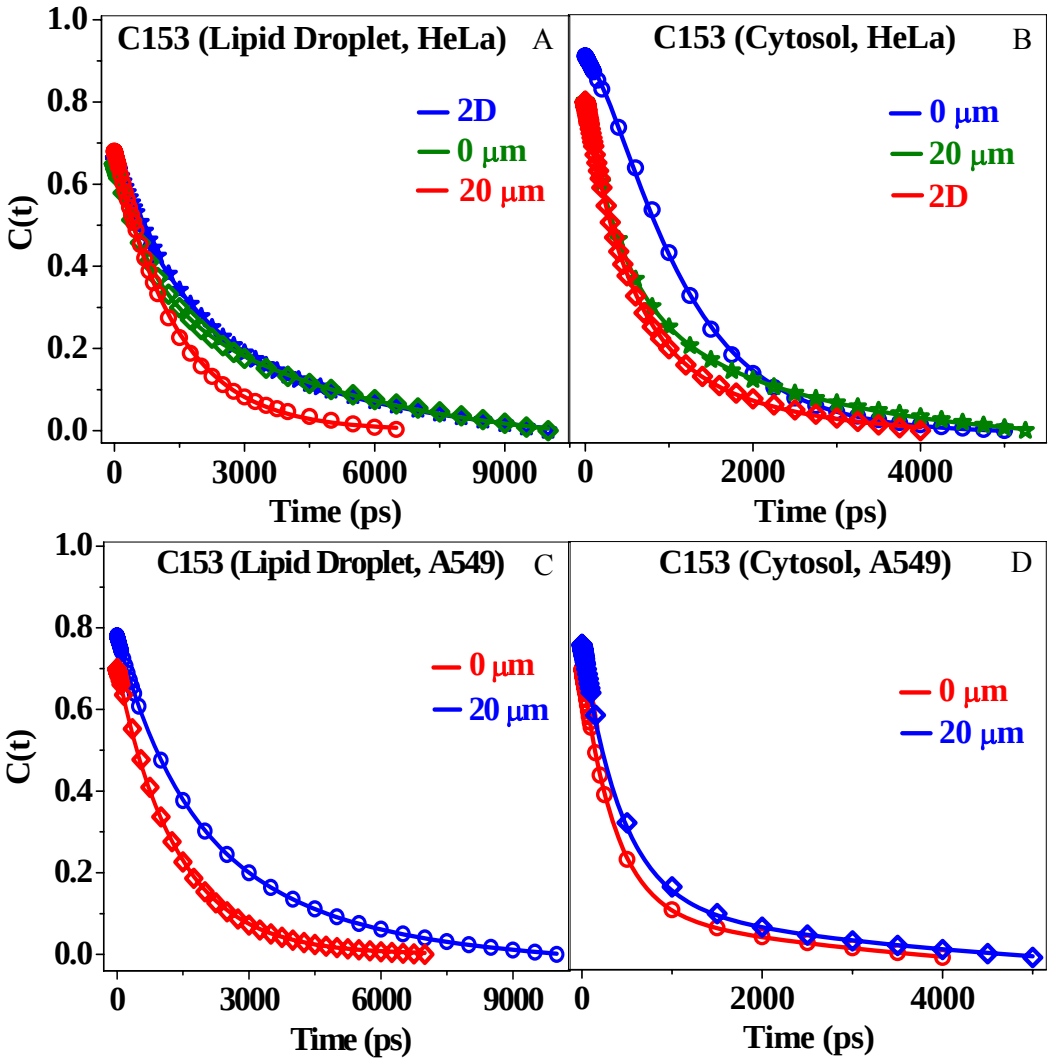

Figure S11. Decay of C(t): C153 inside (A) Lipid droplet and (B) Cytosol of HeLa cell (2D and 3D tumor); (C) Lipid droplet and (D) Cytosol of A549 spheroid. Data points denote values of C(t) and solid lines indicate best fit.

J. Emission Spectra and Corresponding Fluorescence Decays of Dox inside 2D and 3D (Spheroid) A549 Cells

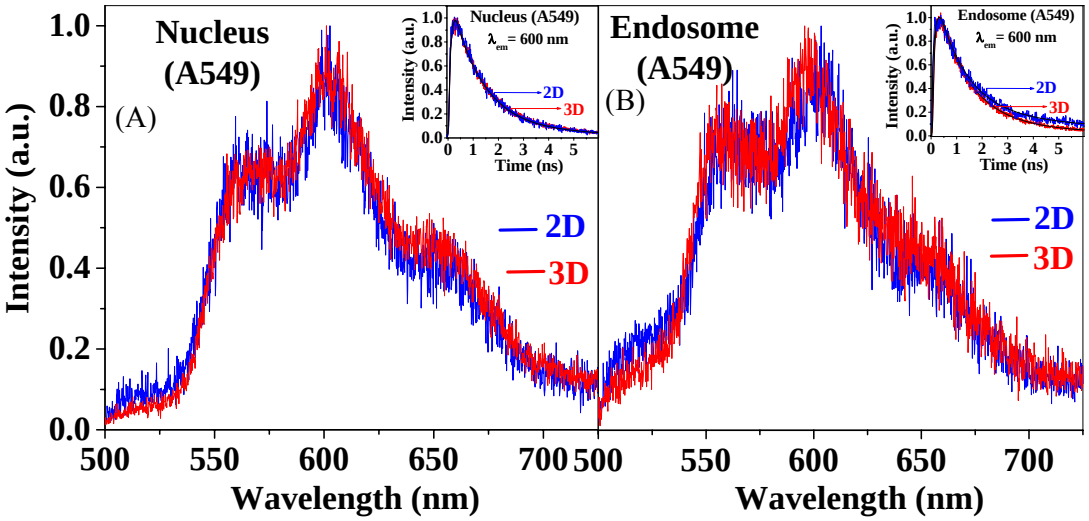

Figure S12. Emission spectra of 2D and 3D (spheroid) A549 cells stained by Dox: (A) Nucleus and (B) Endosomes. Corresponding fluorescence decays (at λ_{em} = 600 nm) are shown in the inset.

References

(1) R. E. M. A. van Herpen, R. J. A. O. Ophuis, M. Wijers, M. B. Bennink, F. A. J. van de Loo, J. Fransen, B. Wieringa and D. G. Wansink, *Mol. Cell Biol.*, 2005, **25**, 1402.

(2) W. Hakamata, S. Tamura, T. Hirano and T. Nishio, *ACS. Med. Chem. Lett.*, 2014, **5**, 321.

(3) R. S. Fee and M. Maroncelli, *Chem. Phys.*, 1994, **183**, 235.

(4) R. Jimenez, G. R. Fleming, P. V. Kumar and M. Maroncelli, *Nature*, 1994, **369**, 471.

(5) M. Maroncelli and G. R. Fleming, *J. Chem. Phys.*, 1987, **86**, 6221.

(6) R. Chowdhury, S. Sen Mojumdar, S. Chattoraj and K. Bhattacharyya, *J. Chem. Phys.*, 2012, **137**, 055104.